






Cooperative virulence via the collective action of secreted pathogen effectors

Received: 7 January 2022

Accepted: 13 January 2023

Published online: 13 February 2023

 Check for updates

Tatiana Ruiz-Bedoya ¹, Pauline W. Wang^{1,2}, Darrell Desveaux ^{1,2,3}  & David S. Guttman ^{1,2,3} 

Although virulence is typically attributed to single pathogenic strains, here we investigated whether effectors secreted by a population of non-virulent strains could function as public goods to enable the emergence of collective virulence. We disaggregated the 36 type III effectors of the phytopathogenic bacterium *Pseudomonas syringae* strain PtoDC3000 into a ‘metaclone’ of 36 coisogenic strains, each carrying a single effector in an effectorless background. Each coisogenic strain was individually unfit, but the metaclone was collectively as virulent as the wild-type strain on *Arabidopsis thaliana*, suggesting that effectors can drive the emergence of cooperation-based virulence through their public action. We show that independently evolved effector suits can equally drive this cooperative behaviour by transferring the effector alleles native to the strain PmaES4326 into the conspecific but divergent strain PtoDC3000. Finally, we transferred the disaggregated PtoDC3000 effector arsenal into *Pseudomonas fluorescens* and show that their cooperative action was sufficient to convert this rhizosphere-inhabiting beneficial bacterium into a phyllosphere pathogen. These results emphasize the importance of microbial community interactions and expand the ecological scale at which disease may be attributed.

Emergent properties of biological systems are higher-order patterns or processes that are irreducible to the individual components of the system, but can arise owing to interactions among those components¹. Examples of emergent properties of bacterial communities include multispecies biofilms that have enhanced antimicrobial resistance, interspecies cross-feeding that result in new metabolic capabilities, plant fitness during host–microbe interactions^{2,3} and, importantly, virulence^{4,5}.


Work from Koch and Henle established postulates for ascribing causative relationships between microorganisms and disease that have resulted in our current understanding that disease is caused by the colonization, growth and dissemination of a single pathogenic organism⁶. Despite the foundational nature of these postulates, they are considered incomplete unless adapted to include the complex and interdependent roles of the host, the environment and

polyclonal (intraspecific) or polymicrobial (interspecific) diversity in the host-associated microbiota^{7,8}.

Although disease can surely be caused by a single pathogenic clone, this clone is usually a member of a diverse microbial community^{7,8}. Infections that encompass these communities have the potential for collective or social behaviours that can result in non-additive, that is, emergent, properties that can change the fitness of individual community members and the ultimate outcome of the interaction. In most cases, microbial social interactions depend on the production of secreted (that is, extracellular) factors that directly or indirectly condition the environment to make it more favourable for microbial growth or persistence.

Secreted factors that promote positive social interactions are called ‘public goods’ as they benefit both the producer of the goods and other individuals in the local vicinity^{9–13}. Strains that produce

¹Department of Cell and Systems Biology, University of Toronto, Toronto, Ontario, Canada. ²Centre for the Analysis of Genome Evolution and Function, University of Toronto, Toronto, Ontario, Canada. ³These authors contributed equally: Darrell Desveaux, David S. Guttman.

 e-mail: darrell.desveaux@utoronto.ca; david.guttman@utoronto.ca

public goods are known as ‘cooperators’ or ‘actors’, whereas those that benefit but do not produce the goods are called ‘recipients’, ‘cheaters’ or ‘freeloaders’^{13,14}. If public goods are costly to produce, recipients will have a competitive advantage over cooperators; however, modelling has shown that cooperators and recipients can coexist even when recipients do not have a fitness advantage^{9,15,16}. Coexistence is particularly likely when cooperation generates immediate mutual fitness benefits to the entire population as happens with the production of iron-scavenging molecules¹¹.

The type III secretion system (T3SS) is a key virulence system used by many extracellular and membrane-associated intracellular pathogens to translocate effectors into host cells to manipulate cellular processes, suppress immunity or acquire nutrients^{17,18}. In plants, T3SS effectors can also elicit effector-trigger immunity (ETI) if the host encodes immune receptors that recognize the presence or activity of specific effectors¹⁹. Consequently, the specific suite of T3SS effectors carried by an individual strain largely determines whether its interaction will result in disease or immunity on a particular host. As extracellular pathogens typically inject their effectors into the host cytosol, their immune-modulatory and/or nutritional benefits can be accrued by all microbes in the vicinity of the breached host cell. Effectors, therefore, have the potential to act as public goods.

Pseudomonas syringae is a bacterial species complex that causes disease in a wide range of plants^{20–22}. The *P. syringae* complex encodes more than 5,000 unique effector proteins in its pangenome, grouped into 70 distinct effector families, with most strains carrying a suite of 12–40 effectors²³. The T3SS and its effectors are required for *P. syringae* virulence²⁴ and T3SS knockout mutant strains can freeloader in a mixed infection with a T3SS wild-type strain and grow to near wild-type levels¹⁶. T3SS-associated freeloader behaviour has also been reported for human pathogens²⁵. Although it is known that a T3SS mutant can benefit from the presence of a T3SS wild-type cooperator, how this translates into a population setting remains unclear.

Here we investigate how the virulence potential of a bacterial population can be modulated by the activity of individual effectors and whether the collective activity of a population can give rise to virulence as an emergent property.

Results

Disaggregation of effectors into a metaclone

To study how suites of effectors and individual effectors modulate host–pathogen interactions, we devised an experimental system to manipulate the effector composition of a strain or population. We disaggregated the repertoire of effectors carried by an individual strain into a metaclone, which comprises a population of coisogenic clones that each express a single effector (Fig. 1a). We produced a metaclone for the 36 T3SS effectors of the tomato and *Arabidopsis thaliana* pathogen *P. syringae* pv. tomato DC3000 (PtoDC3000)²⁶ (Supplementary Table 1). Effectors were barcoded and expressed under the control of their native promoters on a pBBRI-MCS-2 plasmid as previously described²⁶. As T3SS effectors are frequently found on plasmids in situ, plasmid-mediated expression is biologically plausible^{27–39}. We individually transformed each plasmid-borne effector into a PtoDC3000-derived strain in which all 36 effectors had been deleted (PtoDC3000D36E; hereafter designated D36E)⁴⁰. D36E is not virulent and typically grows three or more orders of magnitude less than PtoDC3000 using standard in planta growth assays^{40–43}. We used our library of D36E coisogenic clones expressing individual effectors to set up experiments in which different clones were combined to form equivalent metaclones.

Cooperative virulence via disaggregated effectors

We first tested whether individual PtoDC3000 effectors were sufficient for restoring wild-type levels of virulence when expressed in the effectorless D36E background^{24,40,42,43}. We carried out *A. thaliana* virulence

assays using spray inoculations for each of the 36 PtoDC3000 effectors individually carried by D36E and compared their growth with D36E and the parental PtoDC3000 carrying an empty vector (designated EV). In these assays, bacterial growth is a proxy for virulence. Although there was minor variation in growth across the 36 effector clones, none grew to a level statistically different from D36E in planta (Extended Data Fig. 1). Our results differed slightly from previous studies^{40,42}, in which six individually tested effectors (AvrPtoId, HopAB1j, HopE1a, HopG1c, HopC1a and HopH1a) significantly improved growth in *Nicotiana benthamiana* compared with the D36E empty vector control. These minor differences might be due to our use of native promoters for effector expression compared with the use of a constitutive promoter in those studies, or the use of different plant hosts. We also found that individual effector clones did not vary significantly in their growth in vitro, with all clones having similar growth dynamics (Extended Data Fig. 2).

Next we tested whether the PtoDC3000 metaclone could achieve the same level of virulence as the wild-type PtoDC3000 strain. We reasoned that if no single effector could restore full virulence (Extended Data Fig. 1), the disaggregated effector arsenal of the PtoDC3000 metaclone would only be able to recapitulate PtoDC3000 virulence if part, or all, of the metaclone functioned collectively. We assembled a PtoDC3000 metaclone named D36E::McDC[36], which comprised a population of 36 clones individually expressing, under their native promoter, one of each of the 36 well-expressed PtoDC3000 effectors deleted from D36E. We also assembled a metaclone named D36E::McDC[35], which lacked the effector AvrE1f (Fig. 1b) because previous work had shown that AvrE1f can trigger ETI in *A. thaliana* ecotype Col-0 plants when expressed on a multicopy plasmid²⁶. We spray-infected *A. thaliana* plants with the two metaclones, the parental PtoDC3000 strain and the D36E effectorless strain harbouring empty vectors, and quantified bacterial growth in planta at 3, 5, 7 and 12 days post-infection. The growth of the non-ETI-eliciting metaclone D36E::McDC[35] was indistinguishable from that of the virulent parental strain PtoDC3000::EV, whereas the growth of the ETI-eliciting metaclone D36E::McDC[36] was indistinguishable from the non-virulent D36E::EV (Fig. 1b). We also obtained the same results using a traditional pressure-infiltration pathology assay, which showed that our results were independent of the means of infection (Extended Data Fig. 3). We tracked unique barcode sequences that were incorporated into the effector plasmids to confirm that all individual effector clones within the metaclone were present throughout infection and that the overall diversity of the metaclones remained unchanged (Extended Data Fig. 4). None of the individual effector clones persisted in the population; therefore all, or a subset of, clones acted collectively to promote population fitness. The approximately two log difference in growth between D36E::McDC[36] and D36E::McDC[35] (Fig. 1b) illustrates that effectors that impose a fitness detriment (AvrE1f) can reduce the fitness of the entire population. In other words, immune-eliciting effectors can act as a public bad⁴⁴.

Cooperative virulence enables intra- and inter-specific freeloading

Individual effector clones in a metaclone can only increase their fitness through collective action; therefore, virulence in our experimental system is an emergent property of the metaclone population. It is possible that not all effector clones contribute to metaclone fitness and that some clones could be acting as cheaters or freeloaders. To test whether the collective action of the metaclone was susceptible to exploitation by freeloaders, we investigated whether the metaclone increased the fitness of both the cooperating clones (that is, those clones that contribute public goods to increase in planta microbial fitness) and any freeloader clones (that is, those clones that use but do not provide any public good). To do this, we measured the growth of a freeloading D36E::EV strain when grown in the presence and absence of the metaclone. We measured the

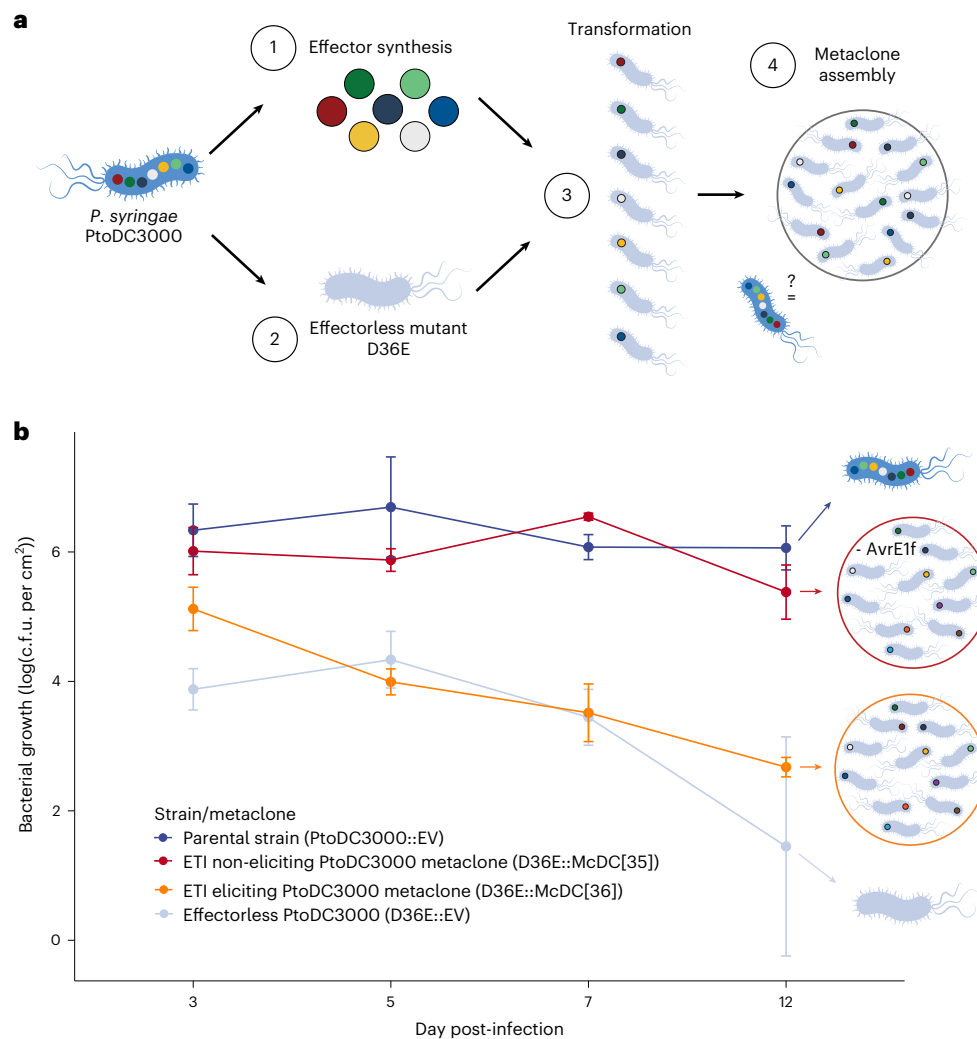


Fig. 1 | Metaclones of *P. syringae* facilitate the emergence of population virulence. **a**, Schematic representation of *P. syringae* metaclone construction. (1) Effector gene sequences of a given parental *P. syringae* strain (PtoDC3000) are annotated, synthesized and cloned into a broad host-range vector. (2) The polymutant strain PtoDC3000D36E (designated D36E), constructed in a previous study⁴⁰, lacks all 36 well-expressed effector genes but retains a functional T3SS. (3) Each synthesized effector is individually transformed into D36E. (4) A library of D36E::effector lines is assembled into a metaclone: a population of isogenic strains that differ only by their carriage of a single effector and that collectively mirrors the effector content of its parental strain. **b**, Virulence of PtoDC3000 is recapitulated collectively by its metaclone on

A. thaliana. In planta bacterial growth measured via spray-infection assays at days 3, 5, 7 and 12 post-infection is shown for the wild-type pathogen PtoDC3000 harbouring an empty vector (PtoDC3000::EV), the effectorless D36E harbouring an empty vector (D36E::EV), an ETI-eliciting D36E metaclone D36E::McDC[36] and a non-ETI-eliciting metaclone lacking AvrE1f, D36E::McDC[35]. Diagrams on the right represent the corresponding population and genetic makeup of each infection. The non-ETI-eliciting metaclone consistently shows higher fitness than its counterpart metaclone capable of mounting a host immune response. Error bars correspond to the standard deviation from the mean of four biological replicates per treatment at each time point. c.f.u., colony-forming unit. Source data provided in Supplementary Data 1.

growth of D36E::EV, PtoDC3000::EV and D36E::McDC[35] individually, and then performed mixed growth assays by combining D36E::EV with either other D36E::EV strains or the D36E::McDC[35] metaclone, maintaining the freeloader strain at the same ratio in the overall population. Different selectable markers were used to distinguish the freeloader fraction from the rest of the population. In both cases, the mixing was done at a 1:36 ratio and growth was determined for the total population and the freeloader fraction (Fig. 2a). The experiment showed that the freeloader D36E::EV had significantly enhanced growth when grown with the D36E::McDC[35] metaclone compared with the control effectorless population (Fig. 2b and Extended Data Fig. 5a). This result indicates that the collective virulence of the metaclone is a synergistic property that can rescue the growth of freeloaders.

We showed that the metaclone can benefit freeloaders that share the same genetic background, but we wanted to know whether the metaclone can benefit entirely unrelated freeloaders, that is, freeloaders

from a different species. To do this, we tested whether the metaclone could enhance the in planta growth of a non-virulent, natural isolate of *P. fluorescens* 0-1 (Pf0-1). The Pf0-1 species is a rhizosphere isolate commonly used in the promotion of plant growth^{45,46}. We spray-infected leaves and measured bacterial density of the total population and the free-living strain via differential selection over 7 days. Pf0-1 alone grew no better than the effectorless D36E strain in *A. thaliana* leaves. However, following co-inoculation with the D36E::McDC[35] metaclone, Pf0-1 in planta growth increased by more than three logs (Fig. 2c and Extended Data Fig. 5b). No significant change in the relative proportion of freeloaders and cooperators was observed, which provides support for the coexistence of all members of the population and the maintenance of the pBBR1MCS-2 plasmid carrying the cloned effectors (Extended Data Fig. 5). These results demonstrate that the public goods provided by the metaclone are available to freeloader strains of both the same and different species in the environment.

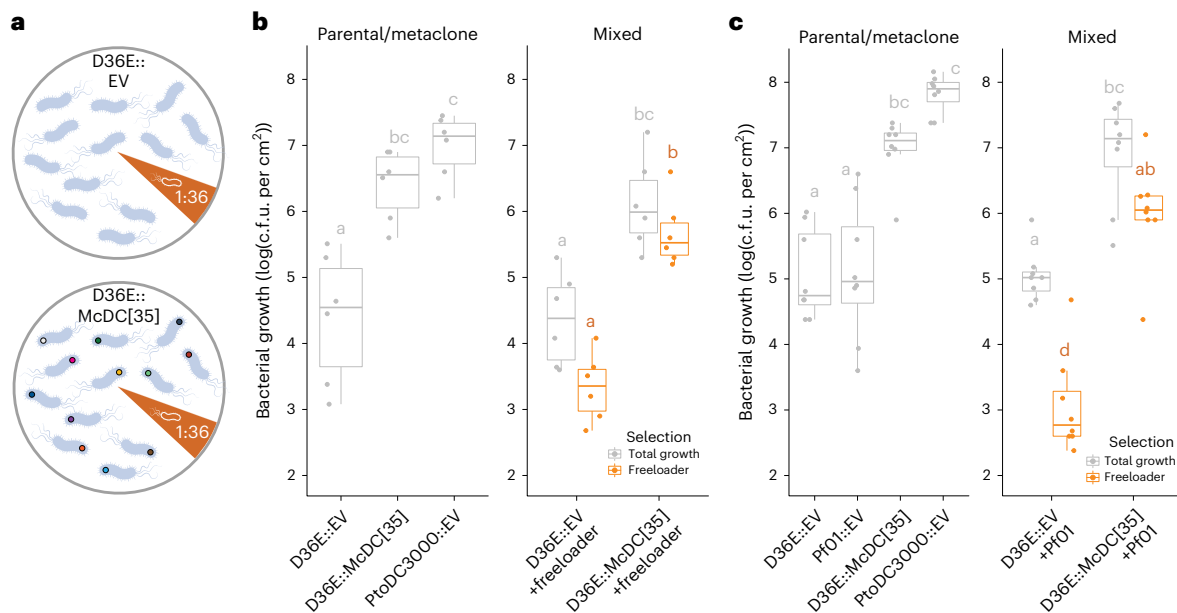


Fig. 2 | Collective action of the PtoDC3000 metaclone supports growth of laboratory and natural freeloader strains. a, Schematics representing the composition of two populations in which an effectorless unfit strain is at a relative abundance of 1:36, shown as the orange wedge. In the cooperating population (bottom), the freeloader is complemented with the metaclone D36E::McDC[35] expressing the effector repertoire of the pathogen PtoDC3000, whereas in the effectorless mock population (top), the freeloader strain is mixed only with D36E harbouring an empty pBBR1MCS-2 vector. **b**, The emergence of collective virulence in the metaclone D36E::McDC[35] ('Mixed' panel) drives a significant increase in fitness of the freeloaded strain (D36E::pUCP20EV, orange) comparative to its performance in the absence of effectors in the control

population. In planta bacterial growth is reported for parental strains, metaclone controls and mixed populations containing the D36E::EV as a test freeloader. **c**, The public goods made available by collective action in the metaclone promote in planta growth of the distantly related *P. fluorescens* natural isolate Pfo1 (Pfo1::pUCP20EV), shown in orange. Growth is reported 7 days post-infection for 6 biological replicates per treatment for total and freeloader growth. Elements in boxplots represent the median, 25th and 75th percentiles and 1.5 \times inter-quantile ranges. All letters represent statistical significance groups, estimated using one-way analysis of variance (ANOVA) and post-hoc Tukey–Kramer honestly significance difference (HSD) comparisons, with a 95% confidence interval. Source data provided in Supplementary Data 1.

Effector arsenals are portable within species

We wanted to test whether the collective virulence we observed was due to coevolution between the effectors and the strain that carries them (that is, expression of PtoDC3000 effectors in the D36E mutant background of PtoDC3000) and whether our results were generalizable to different suites of effectors. Therefore we investigated whether our results could be recapitulated using a metaclone constructed from a suite of effectors carried by a divergent *P. syringae* strain that is able to cause disease on the same host. The use of effectors from another strain has strong biological relevance given the high level of recombination and horizontal gene transfer observed among effectors in the *P. syringae* species complex²⁰. *P. syringae* pv. *maculicola* ES4326 (PmaES4326) is a radish pathogen in phylogroup 5 that is virulent on *A. thaliana* but is divergent from phylogroup 1 strain PtoDC3000 both with respect to its core genome ($d_N = 0.034$; average nucleotide identity (ANI)⁴⁷ = 87.1%) (Fig. 3a) and effector arsenal. At the effector allele level, PtoDC3000 and PmaES4326 carry 36 and 30 alleles with confirmed expression, respectively⁴⁰. Only eight alleles are shared between strains, which results in an allele-level Jaccard similarity value of 0.14 (ref.²³) (Fig. 3b). Similarly, at the effector family level, their combined effector arsenals include 38 out of the 70 distinct *P. syringae* effector families^{23,26}. Of the 38 total families, 16 families were found in both strains, 13 were found only in PtoDC3000 and 9 only in PmaES4326, which results in a family-level Jaccard similarity value of 0.42 (Fig. 3c).

Paralleling the PtoDC3000 metaclones, we created two PmaES4326 metaclones in the D36E background: one with the full complement of effectors, including ETI elicitors, and one without ETI elicitors. Two alleles harboured naturally in PmaES4326 (AvrE1i and HopO1b) have the potential to trigger ETI in *A. thaliana*⁴⁸, so we created an ETI-eliciting metaclone, D36E::McES[30], and a non-ETI eliciting

metaclone, D36E::McES[28] (Fig. 3c). As described above, all effectors were synthesized, cloned and expressed with the native promoters and chaperones when appropriate (Methods). We spray-inoculated the PmaES4326 metaclones and controls onto *A. thaliana* plants and observed similar results to the PtoDC3000 metaclones. That is, the non-ETI-eliciting PmaES4326 metaclone D36E::McES[28] significantly restored in planta growth compared with the effectorless D36E::EV background strain, whereas the ETI-eliciting metaclone D36E::McES[30] did not (Fig. 3d). The most notable difference between the PtoDC3000 and PmaES4326 metaclone experiments was an increased variance between trials. Specifically, the ETI-eliciting PmaES4326 metaclone was significantly more virulent than the D36E::EV background in one experimental replicate. Taken together, these data indicate that the collective action of effectors in a metaclone is functionally independent of the genetic background of conspecific pathogens and effector suits are effectively exchangeable or convergent at relatively large evolutionary distances.

An important hypothesis arising from the PmaES4326 metaclone is whether collective virulence can be explained solely by the set of alleles shared by both PtoDC3000 and PmaES4326. We tested this by creating D36E::McDC&ES[7], which is a population composed of the seven shared alleles between the two strains that do not elicit ETI (Supplementary Table 1). D36E::McDC&ES[7] failed to recover the same population-level virulence observed for D36E::McDC[35] or the parental strain (Extended Data Fig. 6).

Effectors are sufficient for cooperative virulence

Finally, we tested whether an otherwise beneficial species would act as a pathogen after acquiring a disaggregated effector arsenal from a pathogenic species. These experiments tested whether the

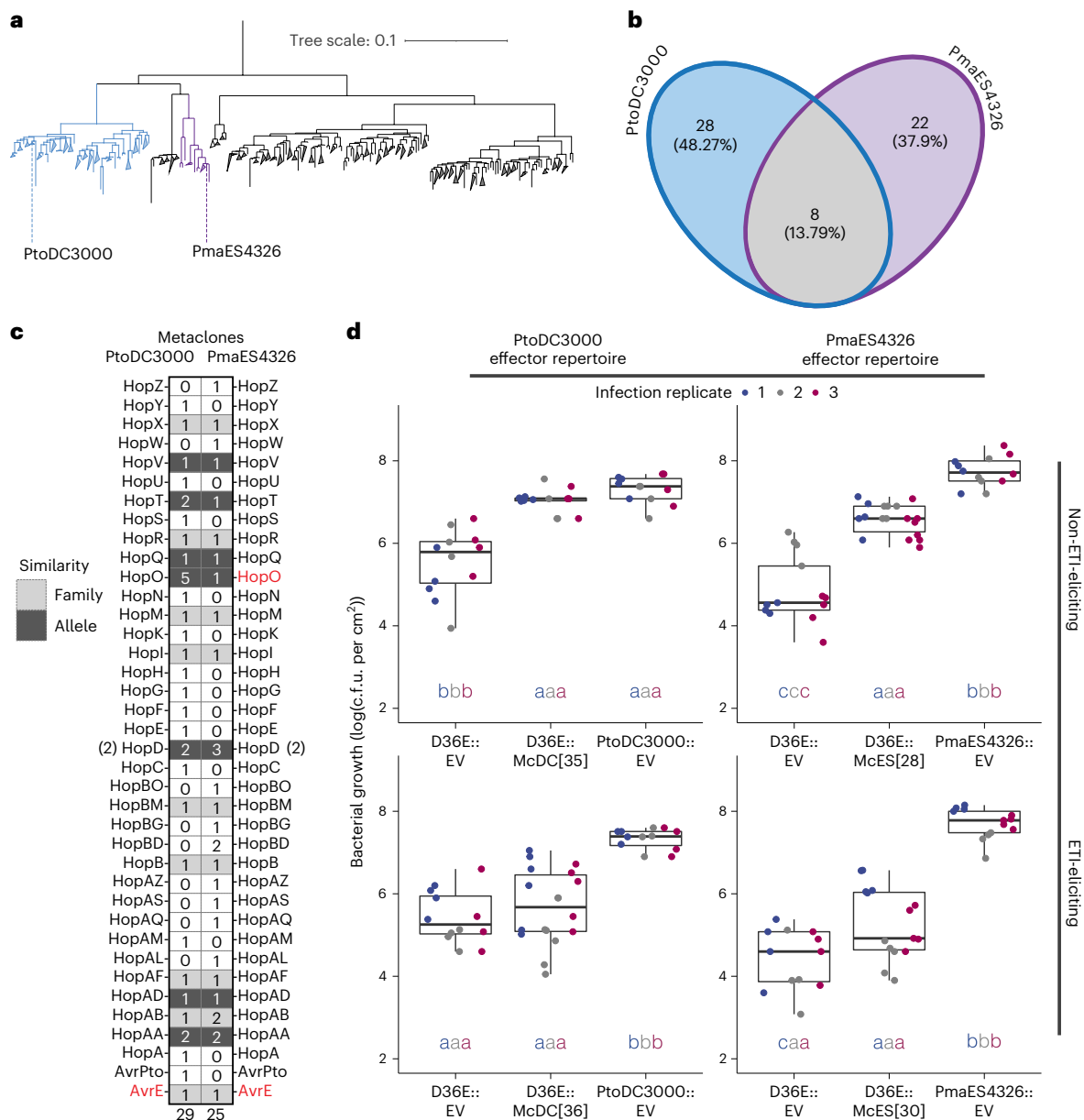


Fig. 3 | Portability of pathogenic effector repertoires. **a**, Core genome, maximum likelihood phylogeny of host-associated strains in the *P. syringae* species complex displays the evolutionary relationship between two pathogens of *A. thaliana*, PtoDC3000 and PmaES4326, clustering in divergent phylogroups 1 (blue) and 5 (purple), respectively. Nodes with distance < 0.01 are collapsed.

b, Venn diagram showing the private and shared effector alleles between PtoDC3000 and PmaES4326 used in this study. **c**, Effector families present in PtoDC3000 and PmaES4326 and used for building their corresponding metaclones. Numbers inside boxes correspond to the total number of unique alleles of each effector family used for metaclone assembly of each strain. Light grey highlighting indicates that the two strains possess different alleles from the same effector family, whereas dark grey indicates allelic identity. Red labelling of an effector indicates a strain-specific ETI-eliciting allele. HopD is marked with (2) as each strain shares two identical alleles. Numbers at the bottom are the sum of unique effector families represented in each genome. Additional information

in Supplementary Table 1. **d**, Effectors native to the genome of PmaES4326 can drive collective virulence when delivered by the distant conspecific relative D36E. In planta bacterial fitness was quantified 6 days post-infection for at least 4 biological replicates per treatment and over 3 independent infection replicates. ETI-eliciting and non-ETI-eliciting D36E metaclones of PtoDC3000 and PmaES4326 were compared with the effectorless strain D36E::EV and their corresponding parental strains carrying empty vectors. Similar to the successful PtoDC3000 metaclone, the non-ETI-eliciting PmaES4326 metaclone D36E::McES[28] reaches collective virulence with significantly higher growth than that of the effectorless D36E strain. Elements in boxplots represent the median, 25th and 75th percentiles and 1.5 \times inter-quartile ranges. All comparisons were performed within each infection replicate. Letters represent significant groups estimated using one-way ANOVA and post hoc Tukey–Kramer HSD comparisons, performed with a confidence level of 95% for 3 independent experiments. Source data provided in Supplementary Data 1.

collective action of effector arsenals is a portable trait between divergent species and whether these effectors are sufficient to enable virulence. Given the complexity of host-associated microbiota and the frequency of horizontal genetic exchange, it is conceivable that effectors could be transmitted across species boundaries. Here we

asked whether these events can fundamentally change the nature of a host–microbe interaction. As discussed above, *P. fluorescens* is a key member of the plant root microbiome that has been widely studied as a plant-growth-promoting species^{45,46}. Although *P. syringae* and *P. fluorescens* are related, the two species are phylogenetically distinct,

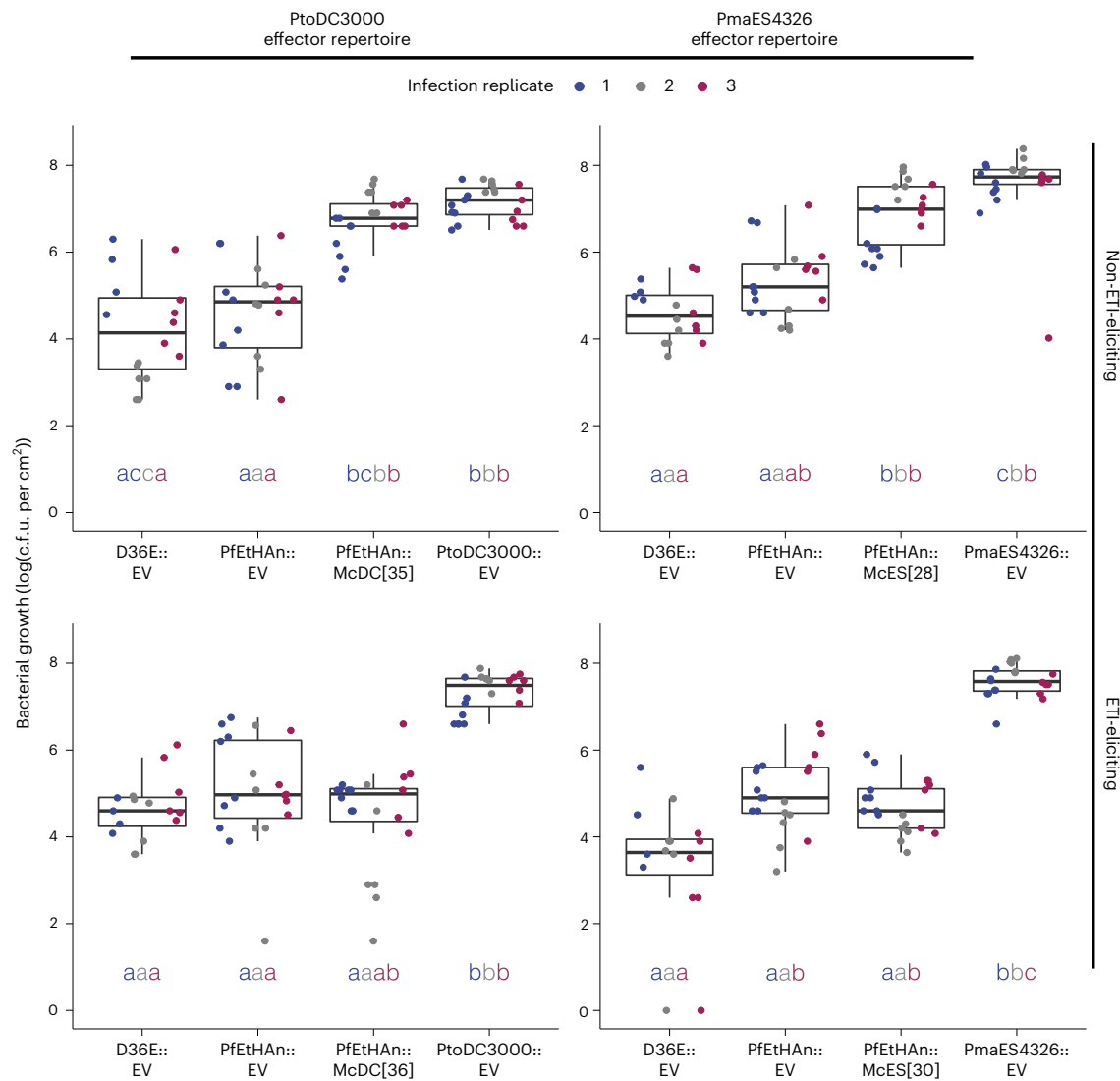


Fig. 4 | Effectors are sufficient for converting a beneficial strain into a pathogen. Metaclones constructed by moving the effectors of PtoDC3000 and PmaES4326 individually into the plant-growth-promoting strain *P. fluorescens* Pf-0 EtHAN (carrying a *P. syringae* T3SS) induce virulence in *A. thaliana*. Three independent spray-infection assays were performed for ETI-eliciting PfEtHAN metaclones PfEtHAN::McDC[36] and PfEtHAN::McES[30], non-ETI-eliciting PfEtHAN metaclones PfEtHAN::McDC[35] and PfEtHAN::McES[28], and control strains harbouring an empty vector. Growth in planta is reported at 6 days

post-infection for at least 4 biological replicates and 3 independent infection replicates. Elements in boxplots represent the median, 25th and 75th percentiles and 1.5× inter-quantile ranges. All comparisons were performed within each infection replicate, and letters represent significance groups estimated using one-way ANOVA and post hoc Tukey–Kramer HSD comparisons were performed with a confidence level of 95% for 3 independent experiments. Source data provided in Supplementary Data 1.

with PtoDC3000 and Pf0-1 sharing an ANI of only 80.73%⁴⁷. This is a similar evolutionary distance to *Escherichia coli* K-12 substr. MG1655 and *Salmonella enterica* subsp. *enterica* serovar Typhimurium str. LT2 (ANI = 81.91%). To test our hypothesis, we used the *P. fluorescens* strain Pf01EtHAN, which has been engineered to contain a functional *P. syringae* T3SS capable of delivering effectors⁴⁹. We individually transformed all PtoDC3000 and PmaES4326 effectors into Pf01EtHAN and assembled ETI-eliciting PfEtHAN::McDC[36] and PfEtHAN::McES[30], and non-ETI-eliciting PfEtHAN::McDC[35] and PfEtHAN::McES[28] metaclones, which represent the effector suites of PtoDC3000 and PmaES4326. We then quantified their growth in planta relative to their corresponding pathogenic parental strains. The non-ETI-eliciting PfEtHAN::McDC[35] metaclone multiplied within the host to levels comparable to those of the pathogen PtoDC3000::EV, whereas the PfEtHAN::McES[28] metaclone grew to a level indistinguishable from PmaES4326::EV (Fig. 4). Consistent

with our observations described above, ETI-eliciting metaclones did not grow significantly better than the effectorless background strains D36E::EV and PfEtHAN::EV. Intermediate virulence and ETI responses were observed in one experimental replicate of non-ETI-eliciting and ETI-eliciting PfEtHAN metaclones. That is, variance in fitness outcomes were moderately higher for the PfEtHAN background than for D36E.

In addition to assessing pathogen fitness by counting the number of viable colonies recovered from in planta growth assays, we assessed plant fitness by monitoring symptom development. Consistent with the results described above, infections with the McDC[35] metaclones developed similar chlorosis to plants infected with the wild-type pathogen PtoDC3000 in both the D36E and the PfEtHAN backgrounds (Extended Data Fig. 7). These data demonstrate that the virulence contribution of effectors is transferrable to different species and that these arsenals (along with the appropriate secretion system) are both portable and sufficient for pathogenicity.

Discussion

Although the importance of interactions within polymicrobial and polyclonal infections are becoming increasingly well recognized, most studies of infectious diseases still focus on the role of single, virulent strains^{7,8}. Here we experimentally showed that virulence can be achieved through collective action, even in the absence of any individually fit strain, making it an emergent property. We demonstrated that effectors act as public goods that can support the growth of other strains in the environment and that functional effector suites can be disaggregated and delivered from multiple strains. We found that effector arsenals are highly portable, can function in independently evolved backgrounds and that the position of a species on the interaction continuum from beneficial to virulent is potentially labile, as a beneficial species can be converted into a pathogen if provided with the appropriate effectors and secretion system. Finally, we showed that a single immune-eliciting effector can negate the fitness benefits of the rest of the effector repertoire; that is, ETI elicitation can be thought of as epistatic or dominant. This finding emphasizes the effectiveness of ETI in limiting disease outbreaks, which is particularly interesting given recent findings that nearly all *P. syringae* strains carry at least one effector with ETI-eliciting potential²⁶. However, pathogens also evolve under tremendous selective pressure to avoid or suppress these ETI responses, which explains the high rate of effector degeneration, loss^{23,50} and the prevalence of ETI-suppressing effectors^{40,42,51–56}.

We propose that all, or a subset, of the clones in a metaculture are cooperators that act synergistically to achieve cooperative virulence. Most studies of cooperation in microbes have been based on centralized sourcing of public goods, wherein one strain incurs the total cost of producing the public good⁵⁷. Here no individual strain pays the cost of producing all the public goods, yet at the same time, no strain is fit without the collective action of multiple strains secreting public goods. This opens questions regarding the distribution of fitness cost/benefits across the population but suggests that ultimately, these public goods provided by multiple members of the community can act together, in support of the reported prevalence of positive interactions among microorganisms^{58,59}.

While effector arsenals might not be naturally found disaggregated among multiple single-effector clones, our study provides evidence for the plausibility of collective action as a mechanism that may contribute to the maintenance of population diversity, the emergence of virulence or host shifts. In accord with the Black Queen hypothesis, it can be advantageous to lose essential yet costly functions (for example, gene products) as long as those functions are produced by other members of the community and are public or leaky⁶⁰. Collective virulence in nature would require the co-occurrence of diverse strains. Although reports of polyclonal and polymicrobial infections are better documented in animal systems than plant systems^{61–63}, cooperation in plant infections has been reported. For example, conspecific *Rhizobium meliloti* strains can promote the establishment of alfalfa nodules⁶⁴ and co-occurrence of multiple *P. syringae* strains in a single host has been recently reported⁶⁵. This finding is somewhat expected given the prevalence of this species, its reputation for long-distance dissemination through the water cycle and its high epiphytic fitness^{21,66}.

It is striking that a plant-growth-promoting rhizosphere-adapted species such as *P. fluorescens* can be converted into a pathogen by the acquisition of so few genes. This is particularly notable given that the spray-inoculation methods required the strains to migrate across the leaf surface to the stomatal openings, transit into the leaf apoplast, move into direct contact with the plant cells, inject effectors and thrive in the apoplastic environment, which presumably is highly different to the rhizosphere where *P. fluorescens* is most frequently found. The interaction spectrum of mutualists to pathogens is clearly fluid, a finding that further supports the challenges in defining “what is a pathogen”⁶⁷. Although debate on this fundamental question has largely focused on the fact that the outcome of a host–microbe interaction

depends on the specific strain, host and environment, our study demonstrated that even relatively small changes in the genetic composition of the microbiota can facilitate certain microbial social behaviours that can result in dramatic changes in the interaction outcome with the host. Although the traditional study of pathogenesis has focused on the virulence potential of individual strains, our study showed that we should incorporate the impact of interactions occurring within these diverse microbial communities.

Methods

Effector selection and synthesis

Effector clones were designed as previously described²⁶. Note that all effector clones were constructed with their native promoters, and chaperones were included when appropriate. All construct sequences were chemically synthesized by Gene Universal and synthesized into a Gateway donor vector harbouring a gentamycin resistance marker (pDONR207). Although PtoDC3000 has 47 annotated effector alleles²³, a number of these are known to be pseudogenes or are poorly expressed. In a previous study⁴⁰, the authors deleted 36 out of the 47 effectors from PtoDC3000 to create the effector polymutant strain D36E, which was used here as the genetic background for the metacultures. We elected to generate clones of only the 36 knocked out PtoDC3000 effectors, as the remaining loci are either weak expressors or pseudogenes and still encoded in the D36E genome. The effector HopT2, deleted in D36E, was not recognized through our methods and was therefore not included in this study. Three HopO alleles deleted from D36E (HopO1-1, HopO1-2 and HopO1-2), correspond to four alleles based on our methods (HopO1a, HopO1b, HopO1c and HopO1d). PmaES4326 has an effector repertoire of 33 effector alleles, of which 3 were excluded from this study owing to lack of expression data (Supplementary Table 1). Of the nine alleles shared by PtoDC3000 and ES4326 (Fig. 3b), eight are well expressed, hence were reported to be deleted from D36E (ref. 40), and seven do not elicit ETI in *A. thaliana* (Supplementary Table 1). For this study, we only considered PtoDC3000 effectors that were deleted or disrupted in the construction of D36E (36 alleles) and effectors of PmaES4326 with expression data available (30 alleles) (Supplementary Table 1 and Fig. 3b,c). The PtoDC3000 effector sequences were synthesized with 100% nucleotide identity to the PtoDC3000 reference genome (NCBI reference sequence identifiers NC_004578.1, NC_004633.1 and NC_004632.1). By contrast, the PmaES4326 effectors were selected from previously synthesized representative alleles in the *P. syringae* Type III Effector Compendium (PsyTEC)²⁶. Each of these 30 PsyTEC representative sequences therefore belong to the same identity cluster as the corresponding sequence native to PmaES4326, which means they share at least 95% nucleotide identity. Selection criteria for representative alleles included the presence of an upstream *hrp* box and no ambiguous bases. One representative (HopBD1g) was selected by chance from the PmaES4326 genome, whereas the remaining 29 representatives were selected from other strains (Supplementary Table 2). No major phenotypic discrepancies are expected between the alleles inside a 95% identity cluster, but minor expression or functional variation cannot be ruled out.

Effector transformation and tri-parental mating

Each pDONR207 vector was transformed into chemically competent *E. coli* DH5 α cells. To confirm insert sizes, plasmids were purified using a Thermo Scientific GeneJet Plasmid Miniprep kit, and NotI sites flanking the construct were targeted for restriction enzyme digestion. Band sizes were confirmed by agarose electrophoresis. Gateway cloning (LR reaction) was performed to transfer the construct insert from the donor vector into a low-copy broad-host-range expression vector (pBBR1MCS-2) with a kanamycin resistance marker, and insert sizes were again confirmed via NotI and EcoRV (from pBBR1MCS-2 backbone) digestions.

Tri-parental mating was used to deliver each of the constructs in pBBR1MCS-2 into either the *P. syringae* polymutant strain D36E or the *P. fluorescens* PfEtHAn strain, with their native rifampicin or tetracycline resistance, respectively. To this end, the strain *E. coli* HB101 (RK600, chloramphenicol resistant) was used as a helper, and double antibiotic selection, including kanamycin, was used to isolate successful colonies after plasmid delivery. Control strains (PtoDC3000::EV, PmaES4326::EV, PfEtHAn::EV and D36E::EV) were built by delivering an empty pBBR1MCS-2 vector into the wild-type strain and consistently maintaining both antibiotics for proper selection. A pUCP20TC non-gateway empty vector was used to construct the both freeloader strains D36E::pUCP20TC(EV) and PF01::pUCP20EV.

Bacterial growth conditions

All *Pseudomonas* spp. strains were grown in selective King's B (KB) agar. Medium was supplemented with antibiotics as follows: 50 $\mu\text{g ml}^{-1}$ of rifampicin for any PtoDC3000 or D36E strain or metaclone; 8 $\mu\text{l ml}^{-1}$ of tetracycline for any strain or metaclone of PfEtHAn; and 100 $\mu\text{g ml}^{-1}$ of streptomycin for PmaES4326. To maintain the plasmid in transformed strains or populations harbouring either a pBBR1MCS-2 or pUCP20TC construct, they were grown in medium additionally supplemented with 50 $\mu\text{g ml}^{-1}$ kanamycin or 8 $\mu\text{l ml}^{-1}$ of tetracycline, respectively. *E. coli* cultures were made with LB medium and supplemented with the appropriate antibiotics.

In vitro bacterial growth assays

Growth curves were performed for D36E::effector lines before assembling the complete D36E::McDC[36] metaclone (Extended Data Fig. 2). Each strain was grown overnight in liquid KB medium with rifampicin and kanamycin. Optical densities (ODs) were measured and adjusted to 0.05 and a starting volume of 150 μl , and cultures were transferred in triplicate to 96-well plates, avoiding edge wells. Growth assays were performed in a microplate reader (ICG12 robot manufactured by S&P Robotics) set to shake and quantify the OD at 600 nm (OD_{600}) every 2 h while maintaining a constant temperature of 30 °C for 60 h (around 10 generations per 24 h).

Plant growth conditions

A. thaliana ecotype Col-0 plants were grown under controlled conditions until ready for infection assays. Seeds were sown into Sunshine Mix 1, LC1 (75–85% sphagnum peat moss, perlite, dolomite, limestone, pH adjusted) and kept under domes until germination. On day 11–15, seedlings were thinned and spaced to avoid overlap at full size. Regular watering and growth chamber conditions (12-h dark photoperiod at 21 °C and 12-h at 20 °C) were maintained until plants reached 3–4 weeks when they were transferred into the laboratory for infection assays.

Metaclone assembly

Individual strains were streaked from –80 °C glycerol stocks and grown overnight in KB agar medium with the corresponding antibiotics at 28 °C. Liquid cultures were inoculated and grown shaking overnight until saturation, when the OD_{600} was measured. If necessary, cell densities were adjusted by spinning down the cultures for 5 min at 4,600 r.p.m. and correcting their final volume to reach equal concentrations. For any given metaclone, equal volumes of individual strains were mixed to produce a single liquid culture with all corresponding antibiotics, which was then vortexed at low speed until thoroughly mixed and stocked or plated. Note that for instances in which more than one allele of the same cluster (for example, HopR1g) was annotated and included in this study, the final concentration of its corresponding D36E or PfEtHAn metaclone was adjusted accordingly.

Spray-infection assays

All strains and metaclones used for spray-inoculation assays were taken through two growth cycles to help synchronize growth and to

guarantee that infections were made with fresh culture. A first streak from –80 °C glycerol stocks in the corresponding antibiotics was followed by 30–48 h of growth at room temperature. Subsequently, bacteria were resuspended in 10 mM MgSO_4 and streaked onto fresh plates to form lawns. For metaclones, either fresh well-mixed liquid culture was plated or full cryovial stocks were thawed and immediately plated. Heavy metaclone lawns were recovered by adding 4 ml of 1 \times KB medium and shaking the plates at 1,700 r.p.m. A final solution of 1:100 was prepared, plated and grown at 28 °C for infection. When ready for spray infection, strains and metaclones were recovered from plates, resuspended in a solution of 10 mM MgSO_4 with 0.04% Silwet L-77, and were sprayed at an $\text{OD}_{600} = 2$. This inoculum concentration was chosen after testing a range of $\text{OD}_{600} = 0.5\text{--}4$, with similar visual results across the range (Extended Data Fig. 8). Approximately 2.5 ml of bacterial solution was sprayed onto each plant using Preval sprayers. Immediately after spraying, plants were domed to maintain consistent humidity conditions until the completion of each experiment. The progression of disease was monitored using bacterial growth assays. Day 0 measurements of OD_{600} were taken with the purpose of adjusting to the desired value and are not included in figures as they represent the sprayed solution and not in planta growth.

Leaf syringe infiltration assays

Similar to spray infections, syringe-pressure infiltrations were performed with strains or populations at active log phase, grown overnight in solid KB medium supplemented with their corresponding antibiotics. On the day of infection, plants were marked and domed at least 1 h before infection to incentivize stomatal opening. All bacterial treatments were resuspended in 10 mM MgSO_4 and diluted to reach a final $\text{OD}_{600} = 0.00002$. Using 1 cc needleless sterile syringes, leaves were pressure infiltrated, and excess moisture was cleaned. After infection, plants were domed for 1 h, after which day 0 measurements were taken. Plants were returned to their growth chamber conditions and undomed until collected at the indicated time point.

In planta growth assays

Following spray or pressure-infiltration infections, in planta growth assays were carried out to quantify endophytic bacterial fitness. For each infected plant, tissue was collected from a total of four leaves, which were cleaned to remove excess moisture before coring. An area of 1 cm^2 was collected from each leaf using a number 3 corer. Four cores (4 leaves from 1 plant) were pooled together and sterilized with 70% ethanol for 10 s to remove epiphytes in control experiments. All 4 harvested cores per plant (typically 5 plants per treatment) were then transferred together into 200 μl of 10 mM MgSO_4 with a sterile glass bead. Samples were ground in a bead-beater for 2 min to release and recover endophytic bacterial cells residing in the apoplast. The plant–microbe solution was then transferred to the top row of a 96 well-plate, and 10-fold serial dilutions were performed by transferring 20 μl of 10 mM MgSO_4 into wells with 180 μl of the same MgSO_4 solution. Next, 5 μl of solution across dilutions were plated on solid KB medium with the native antibiotic of the corresponding strain or population. Colony counts were performed after 24–48 h of growth at 30 °C, and bacterial fitness results are reported as $\log(\text{colony-forming units per cm}^2)$. All bacterial growth data were analysed using Rstudio (v.1.3.1073), and the following packages were used: ggplot2 (v.3.3.5), readr (v.2.1.1), RColorBrewer (v.1.1-2), ggsci (v.2.9), ggpubr (v.0.4.0) and scales (v.1.1.1).

Effector barcode amplification, sequencing and quantification

Effector-specific barcodes were obtained directly from infected leaves via PCR. Primers were designed on the basis of the final pBBR1MCS-2 broad-host-range vector containing the synthesized constructs. All barcodes were 8-bp long and at least one mutational step away from each other²⁶. Primers were designed to include Nextera overhang

adapters to enable manageable high-throughput library preparation (Supplementary Table 3) and to produce an amplicon of approximate 300 bp, which only differs across all constructs in their barcode sequence. A modified Dilution and Storage protocol using Thermo Scientific Phire Plant Direct PCR was optimized to enable storage of the plant–microbe solution obtained during in planta bacterial growth assays for subsequent amplification. This strategy was optimized so that amplicon concentrations reflected bacterial densities used for infection to a recovery threshold at $OD_{600} = 0.002$. Effector composition of metaclones in sequencing data followed expectations based on the initial molarity of individual effectors in the inoculum. Tissue samples were stored at $-20\text{ }^{\circ}\text{C}$. A two-step, short-cycle PCR reaction was optimized to avoid PCR bias as follows: initial denaturation for 5 min at $98\text{ }^{\circ}\text{C}$; 24 cycles of 5 s at $98\text{ }^{\circ}\text{C}$ followed by extension for 5 s at $72\text{ }^{\circ}\text{C}$; and 1 min at $72\text{ }^{\circ}\text{C}$. Amplicons were column-cleaned using Macherey–Nagel NucleoSpin Gel and PCR Clean-up and sent for Next-Seq Illumina 150 paired-end sequencing at the Center for the Analysis of Genome Evolution and Function. Trimmomatic (v.0.38)⁶⁸ was used to remove sequencing adapters, filter (-phred33) and set minimal length (MINLEN:100). Finally, an in-house custom Python script using Biopython⁶⁹ (v.1.79, Seq, SeqIO), was used to quantify effector-specific barcode sequences. These counts were used to calculate mean Shannon index values, which represent effector-clone diversity (vegan (v.2.5-7)⁷⁰ in RStudio (v.1.3.1073)).

Freeloader experiment

For each public good experiment (Fig. 2 and Extended Data Fig. 5), the mixed populations (Fig. 2a) were assembled by inoculating KB broth liquid cultures supplemented with rifampicin only and incubating overnight at $30\text{ }^{\circ}\text{C}$ and shaking until saturation. Cultures were spun down and OD_{600} was normalized across all clones before mixing. All populations containing a test freeloader strain were mixed in a 1:36 ratio (freeloader:rest of the population), both when mixed with the metaclones and when mixed with a mock population. Metaclone assembly conditions were followed downstream, keeping only rifampicin selection before infection to avoid excluding either genotype of the mix. For the mock metaclone, D36E harbouring an empty pBBR1MCS-2 was used as a background effectorless mock and was mixed with the test freeloader (D36E harbouring a pUCP20TC empty vector or *P. fluorescens* Pf0-1 harbouring the same empty vector, both with tetracycline resistance). A similar process was followed to construct the metaclone mixed populations, in which each clone of D36E::McDC[35] was mixed in at the same concentration as the test freeloader. The resulting freeloader ratio (tetracycline resistance) was therefore 1:36 for both the mock and the metaclone mixed populations. Spray infections and growth assays were performed as described above, but with differential selection of the tenfold serial dilution in rifampicin alone (no selection, total growth), rifampicin plus kanamycin (selection for pBBR1MCS-2, metaclone/background mock) and rifampicin plus tetracycline (selection for pUCP20TC, freeloader).

Statistics

To evaluate differences in growth between strains and metaclones, analysis of variance (ANOVA) tests were performed with post-hoc Tukey or Tukey–Kramer honestly significant difference tests using 95% confidence intervals. All data processing was performed in RStudio (v.1.3.1073), using packages in tidyverse (v.1.3.1), ggpubr (v.0.4.0) and multcompView (v.0.1-8) for significant grouping. Source data and statistical analyses for all main figures are reported in Supplementary Data 1.

Reporting summary

Further information on research design is available in the Nature Portfolio Reporting Summary linked to this article.

Data availability

Metaclone data are available in Supplementary Data 1. Barcode sequence data are available at <https://doi.org/10.5281/zenodo.7254975>.

Code availability

The script used for reading metaclone barcodes is available at <https://doi.org/10.5281/zenodo.7249118> (<https://zenodo.org/record/7249118>).

References

1. Mayr, E. *The Growth of Biological Thought: Diversity, Evolution, and Inheritance* (Belknap Press, 1982).
2. Afkhami, M. E. & Stinchcombe, J. R. Multiple mutualist effects on genomewide expression in the tripartite association between *Medicago truncatula*, nitrogen-fixing bacteria and mycorrhizal fungi. *Mol. Ecol.* **25**, 4946–4962 (2016).
3. Shalev, O. et al. Commensal *Pseudomonas* strains facilitate protective response against pathogens in the host plant. *Nat. Ecol. Evol.* **6**, 383–396 (2022).
4. Flemming, H. C. et al. Biofilms: an emergent form of bacterial life. *Nat. Rev. Microbiol.* **14**, 563–575 (2016).
5. Casadevall, A., Fang, F. C. & Pirofski, L. A. Microbial virulence as an emergent property: consequences and opportunities. *PLoS Pathog.* **7**, e1002136 (2011).
6. Hanson, R. P. Koch is dead. *J. Wildl. Dis.* **24**, 193–200 (1988).
7. Falkow, S. Molecular Koch's postulates applied to bacterial pathogenicity—a personal recollection 15 years later. *Nat. Rev. Microbiol.* **2**, 67–72 (2004).
8. Vonaesch, P., Anderson, M. & Sansonetti, P. J. Pathogens, microbiome and the host: emergence of the ecological Koch's postulates. *FEMS Microbiol. Rev.* **42**, 273–292 (2018).
9. Friesen, M. L. Social evolution and cheating in plant pathogens. *Annu. Rev. Phytopathol.* **58**, 55–75 (2020).
10. Smith, J. The social evolution of bacterial pathogenesis. *Proc. Biol. Sci.* **268**, 61–69 (2001).
11. Smith, P. & Schuster, M. Public goods and cheating in microbes. *Curr. Biol.* **29**, R442–R447 (2019).
12. West, S. A., Diggle, S. P., Buckling, A., Gardner, A. & Griffin, A. S. The social lives of microbes. *Annu. Rev. Ecol. Evol. Syst.* **38**, 53–77 (2007).
13. West, S. A., Griffin, A. S., Gardner, A. & Diggle, S. P. Social evolution theory for microorganisms. *Nat. Rev. Microbiol.* **4**, 597–607 (2006).
14. Riehl, C. & Frederickson, M. E. Cheating and punishment in cooperative animal societies. *Philos. Trans. R. Soc. Lond. B Biol. Sci.* **371**, 20150090 (2016).
15. West, S. A. & Buckling, A. Cooperation, virulence and siderophore production in bacterial parasites. *Proc. Biol. Sci.* **270**, 37–44 (2003).
16. Barrett, L. G., Bell, T., Dwyer, G. & Bergelson, J. Cheating, trade-offs and the evolution of aggressiveness in a natural pathogen population. *Ecol. Lett.* **14**, 1149–1157 (2011).
17. Buttner, D. Behind the lines—actions of bacterial type III effector proteins in plant cells. *FEMS Microbiol. Rev.* **40**, 894–937 (2016).
18. Khan, M., Seto, D., Subramaniam, R. & Desveaux, D. Oh, the places they'll go! A survey of phytopathogen effectors and their host targets. *Plant J.* **93**, 651–663 (2018).
19. Jones, J. D. & Dangl, J. L. The plant immune system. *Nature* **444**, 323–329 (2006).
20. Dillon, M. M. et al. Recombination of ecologically and evolutionarily significant loci maintains genetic cohesion in the *Pseudomonas syringae* species complex. *Genome Biol.* **20**, 3 (2019).
21. Morris, C. E., Monteil, C. L. & Berge, O. The life history of *Pseudomonas syringae*: linking agriculture to earth system processes. *Annu. Rev. Phytopathol.* **51**, 85–104 (2013).

22. Xin, X. F., Kvitko, B. & He, S. Y. *Pseudomonas syringae*: what it takes to be a pathogen. *Nat. Rev. Microbiol.* **16**, 316–328 (2018).
23. Dillon, M. M. et al. Molecular evolution of *Pseudomonas syringae* type III secreted effector proteins. *Front. Plant Sci.* **10**, 418 (2019).
24. Cunnac, S. et al. Genetic disassembly and combinatorial reassembly identify a minimal functional repertoire of type III effectors in *Pseudomonas syringae*. *Proc. Natl Acad. Sci. USA* **108**, 2975–2980 (2011).
25. Rundell, E. A., McKeithen-Mead, S. A. & Kazmierczak, B. I. Rampant cheating by pathogens? *PLoS Pathog.* **12**, e1005792 (2016).
26. Laflamme, B. et al. The pan-genome effector-triggered immunity landscape of a host–pathogen interaction. *Science* **367**, 763–768 (2020).
27. Yucel, I. et al. Avirulence gene *avrPphC* from *Pseudomonas syringae* pv. *phaseolicola* 3121: a plasmid-borne homolog of *avrC* closely linked to an *avrD* allele. *Mol. Plant Microbe Interact.* **7**, 677–679 (1994).
28. Jackson, R. W. et al. Identification of a pathogenicity island, which contains genes for virulence and avirulence, on a large native plasmid in the bean pathogen *Pseudomonas syringae* pathovar *phaseolicola*. *Proc. Natl Acad. Sci. USA* **96**, 10875–10880 (1999).
29. Tsiamis, G. et al. Cultivar-specific avirulence and virulence functions assigned to *avrPphF* in *Pseudomonas syringae* pv. *phaseolicola*, the cause of bean halo-blight disease. *EMBO J.* **19**, 3204–3214 (2000).
30. Jackson, R. W. et al. Location and activity of members of a family of virPphA homologues in pathovars of *Pseudomonas syringae* and *P. savastanoi*. *Mol. Plant Pathol.* **3**, 205–216 (2002).
31. Buell, C. R. et al. The complete genome sequence of the *Arabidopsis* and tomato pathogen *Pseudomonas syringae* pv. *tomato* DC3000. *Proc. Natl Acad. Sci. USA* **100**, 10181–10186 (2003).
32. Rohmer, L., Kjemtrup, S., Marchesini, P. & Dangl, J. L. Nucleotide sequence, functional characterization and evolution of pFKN, a virulence plasmid in *Pseudomonas syringae* pathovar *maculicola*. *Mol. Microbiol.* **47**, 1545–1562 (2003).
33. Stavrinos, J. & Guttman, D. S. Nucleotide sequence and evolution of the five-plasmid complement of the phytopathogen *Pseudomonas syringae* pv. *maculicola* ES4326. *J. Bacteriol.* **186**, 5101–5115 (2004).
34. Sundin, G. W. et al. Complete nucleotide sequence and analysis of pPSR1 (72,601 bp), a pPT23A-family plasmid from *Pseudomonas syringae* pv. *syringae* A2. *Mol. Genet. Genomics* **270**, 462–476 (2004).
35. Joardar, V. et al. Whole-genome sequence analysis of *Pseudomonas syringae* pv. *phaseolicola* 1448A reveals divergence among pathovars in genes involved in virulence and transposition. *J. Bacteriol.* **187**, 6488–6498 (2005).
36. Zhao, Y., Ma, Z. & Sundin, G. W. Comparative genomic analysis of the pPT23A plasmid family of *Pseudomonas syringae*. *J. Bacteriol.* **187**, 2113–2126 (2005).
37. Perez-Martinez, I., Zhao, Y., Murillo, J., Sundin, G. W. & Ramos, C. Global genomic analysis of *Pseudomonas savastanoi* pv. *savastanoi* plasmids. *J. Bacteriol.* **190**, 625–635 (2008).
38. Baltrus, D. A. et al. Dynamic evolution of pathogenicity revealed by sequencing and comparative genomics of 19 *Pseudomonas syringae* isolates. *PLoS Pathog.* **7**, e1002132 (2011).
39. Gutierrez-Barranquero, J. A., Cazorla, F. M., de Vicente, A. & Sundin, G. W. Complete sequence and comparative genomic analysis of eight native *Pseudomonas syringae* plasmids belonging to the pPT23A family. *BMC Genomics* **18**, 365 (2017).
40. Wei, H. L. et al. *Pseudomonas syringae* pv. *tomato* DC3000 type III secretion effector polymutants reveal an interplay between HopAD1 and AvrPtoB. *Cell Host Microbe* **17**, 752–762 (2015).
41. Chakravarthy, S., Worley, J. N., Montes-Rodriguez, A. & Collmer, A. *Pseudomonas syringae* pv. *tomato* DC3000 polymutants deploying coronatine and two type III effectors produce quantifiable chlorotic spots from individual bacterial colonies in *Nicotiana benthamiana* leaves. *Mol. Plant Pathol.* **19**, 935–947 (2018).
42. Wei, H. L., Zhang, W. & Collmer, A. Modular study of the type III effector repertoire in *Pseudomonas syringae* pv. *tomato* DC3000 reveals a matrix of effector interplay in pathogenesis. *Cell Rep.* **23**, 1630–1638 (2018).
43. Wei, H. L. & Collmer, A. Defining essential processes in plant pathogenesis with *Pseudomonas syringae* pv. *tomato* DC3000 disarmed polymutants and a subset of key type III effectors. *Mol. Plant Pathol.* **19**, 1779–1794 (2018).
44. Engel, C. Scientific disintegrity as a public bad. *Perspect. Psychol. Sci.* **10**, 361–379 (2015).
45. Silby, M. W. et al. Genomic and genetic analyses of diversity and plant interactions of *Pseudomonas fluorescens*. *Genome Biol.* **10**, R51 (2009).
46. Haney, C. H., Samuel, B. S., Bush, J. & Ausubel, F. M. Associations with rhizosphere bacteria can confer an adaptive advantage to plants. *Nat. Plants* **1**, 15051 (2015).
47. Goris, J. et al. DNA–DNA hybridization values and their relationship to whole-genome sequence similarities. *Int. J. Syst. Evol. Microbiol.* **57**, 81–91 (2007).
48. Martel, A. et al. Metaeffector interactions modulate the type III effector-triggered immunity load of *Pseudomonas syringae*. *PLoS Pathog.* **18**, e1010541 (2022).
49. Thomas, W. J., Thireault, C. A., Kimbrel, J. A. & Chang, J. H. Recombineering and stable integration of the *Pseudomonas syringae* pv. *syringae* 61 hrp/hrc cluster into the genome of the soil bacterium *Pseudomonas fluorescens* Pf0-1. *Plant J.* **60**, 919–928 (2009).
50. Stavrinos, J., Ma, W. & Guttman, D. S. Terminal reassortment drives the quantum evolution of type III effectors in bacterial pathogens. *PLoS Pathog.* **2**, e104 (2006).
51. Kim, H. S. et al. The *Pseudomonas syringae* effector AvrRpt2 cleaves its C-terminally acylated target, RIN4, from *Arabidopsis* membranes to block RPM1 activation. *Proc. Natl Acad. Sci. USA* **102**, 6496–6501 (2005).
52. Ritter, C. & Dangl, J. L. Interference between two specific pathogen recognition events mediated by distinct plant disease resistance genes. *Plant Cell* **8**, 251–257 (1996).
53. Jamir, Y. et al. Identification of *Pseudomonas syringae* type III effectors that can suppress programmed cell death in plants and yeast. *Plant J.* **37**, 554–565 (2004).
54. Guo, M., Tian, F., Wamboldt, Y. & Alfano, J. R. The majority of the type III effector inventory of *Pseudomonas syringae* pv. *tomato* DC3000 can suppress plant immunity. *Mol. Plant Microbe Interact.* **22**, 1069–1080 (2009).
55. Gimenez-Ibanez, S. et al. Differential suppression of *Nicotiana benthamiana* innate immune responses by transiently expressed *Pseudomonas syringae* type III effectors. *Front. Plant Sci.* **9**, 688 (2018).
56. Wilton, M. et al. The type III effector HopF2Pto targets *Arabidopsis* RIN4 protein to promote *Pseudomonas syringae* virulence. *Proc. Natl Acad. Sci. USA* **107**, 2349–2354 (2010).
57. Cressler, C. E., Mc, L. D., Rozins, C., J, V. D. H. & Day, T. The adaptive evolution of virulence: a review of theoretical predictions and empirical tests. *Parasitology* **143**, 915–930 (2016).
58. Ona, L. et al. Obligate cross-feeding expands the metabolic niche of bacteria. *Nat. Ecol. Evol.* **5**, 1224–1232 (2021).
59. Kehe, J. et al. Positive interactions are common among culturable bacteria. *Sci. Adv.* **7**, eabi7159 (2021).

60. Morris, J. J., Lenski, R. E. & Zinser, E. R. The Black Queen Hypothesis: evolution of dependencies through adaptive gene loss. *mBio* <https://doi.org/10.1128/mBio.00036-12> (2012).
61. Lamichhane, J. R. & Venturi, V. Synergisms between microbial pathogens in plant disease complexes: a growing trend. *Front. Plant Sci.* **6**, 385 (2015).
62. Rodrigues, L. M. R., Sera, G. H., Filho, O. G., Beriam, L. O. S. & de Almeida, I. M. G. First report of mixed infection by *Pseudomonas syringae* pathovars *garcae* and *tabaci* on coffee plantations. *Bragantia* **74**, 543–549 (2017).
63. Karasov, T. L. et al. *Arabidopsis thaliana* and *Pseudomonas* pathogens exhibit stable associations over evolutionary timescales. *Cell Host Microbe* **24**, 168–179.e4 (2018).
64. Kapp, D., Niehaus, K., Quandt, J., Muller, P. & Puhler, A. Cooperative action of *Rhizobium meliloti* nodulation and infection mutants during the process of forming mixed infected alfalfa nodules. *Plant Cell* **2**, 139–151 (1990).
65. Morris, C. E. et al. *Pseudomonas syringae* on plants in Iceland has likely evolved for several million years outside the reach of processes that mix this bacterial complex across Earth's temperate zones. *Pathogens* **11**, 357 (2022).
66. Arnold, D. L. & Preston, G. M. *Pseudomonas syringae*: enterprising epiphyte and stealthy parasite. *Microbiology (Reading)* **165**, 251–253 (2019).
67. Casadevall, A. & Pirofski, L. A. What is a pathogen? *Ann. Med.* **34**, 2–4 (2002).
68. Bolger, A. M., Lohse, M. & Usadel, B. Trimmomatic: a flexible trimmer for Illumina sequence data. *Bioinformatics* **30**, 2114–2120 (2014).
69. Cock, P. J. et al. Biopython: freely available Python tools for computational molecular biology and bioinformatics. *Bioinformatics* **25**, 1422–1423 (2009).
70. Oksanen, J. et al. vegan: Community Ecology Package. R package version 2.6-4 <http://cran.r-project.org/web/packages/vegan/index.html> (2011).

Acknowledgements

We thank the members of the Desveaux and Guttman laboratories for their advice and feedback throughout this project, with particular thanks to A. Martel for his assistance with strain transformations and to M. Dillon for his insights into effector extraction and construct synthesis. We would also like to thank and acknowledge A. Collmer and J. Chang for providing us with the strains PtoDC3000D36E (that is, D36E, CUCPB6119) and PfEtHAN, which were invaluable

to this study. This project is supported by Natural Sciences and Engineering Research Council of Canada (NSERC) Discovery Grants (to D.S.G. and D.D.).

Author contributions

T.R.-B., D.D. and D.S.G. designed the project. T.R.-B. performed transformations, tri-parental matings, metaclone constructions, spray infections, in planta and in vitro growth assays, primer design, barcode quantification and analysed the data. P.W.W. generated sequence data and assisted with many aspects of the project. T.R.-B., D.D. and D.S.G. wrote the paper. All authors reviewed and agreed on the manuscript.

Competing interests

The authors declare no competing interests.

Additional information

Extended data is available for this paper at <https://doi.org/10.1038/s41564-023-01328-8>.

Supplementary information The online version contains supplementary material available at <https://doi.org/10.1038/s41564-023-01328-8>.

Correspondence and requests for materials should be addressed to Darrell Desveaux or David S. Guttman.

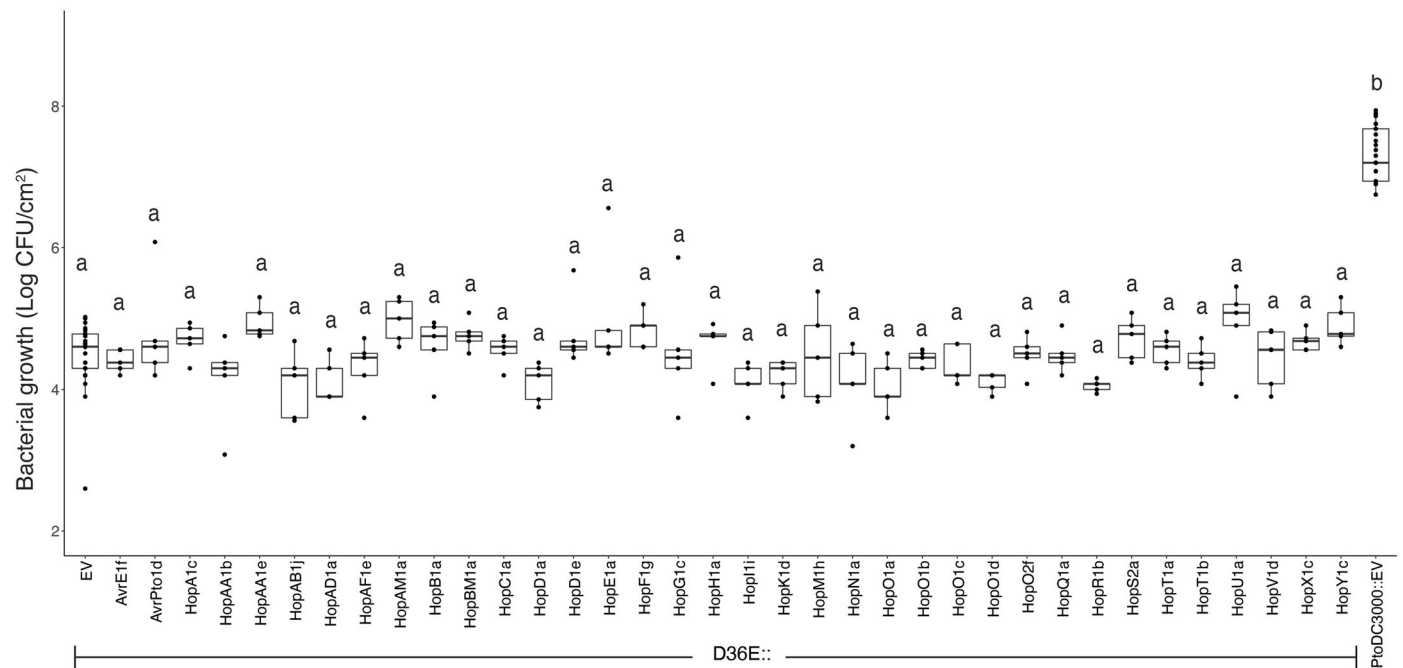
Peer review information *Nature Microbiology* thanks Maren Friesen, John Mansfield, Hai-Lei Wei and the other, anonymous, reviewer(s) for their contribution to the peer review of this work.

Reprints and permissions information is available at www.nature.com/reprints.

Publisher's note Springer Nature remains neutral with regard to jurisdictional claims in published maps and institutional affiliations.

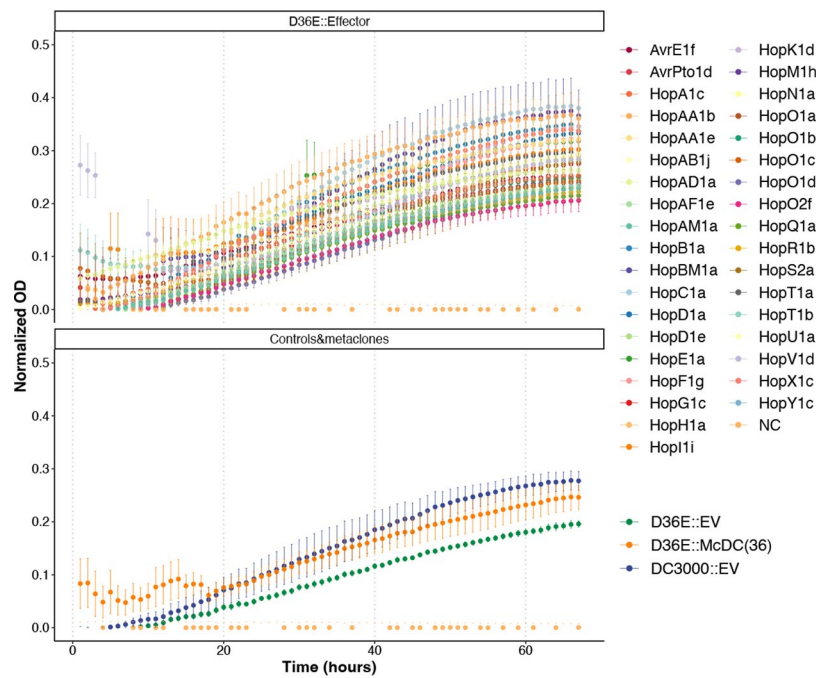
Springer Nature or its licensor (e.g. a society or other partner) holds exclusive rights to this article under a publishing agreement with the author(s) or other rightsholder(s); author self-archiving of the accepted manuscript version of this article is solely governed by the terms of such publishing agreement and applicable law.

© The Author(s), under exclusive licence to Springer Nature Limited 2023



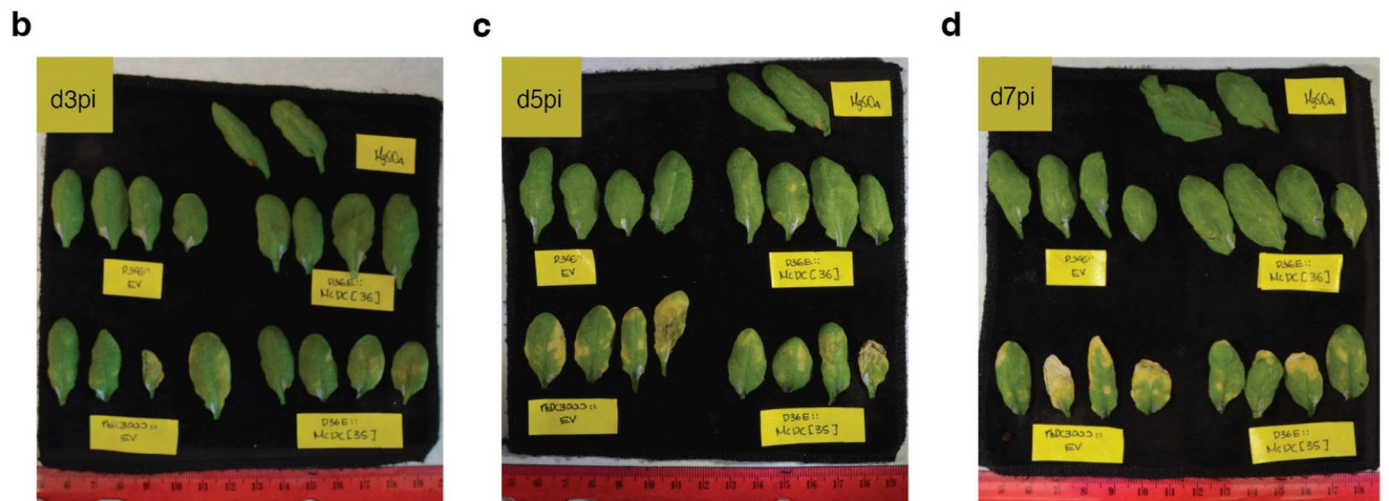
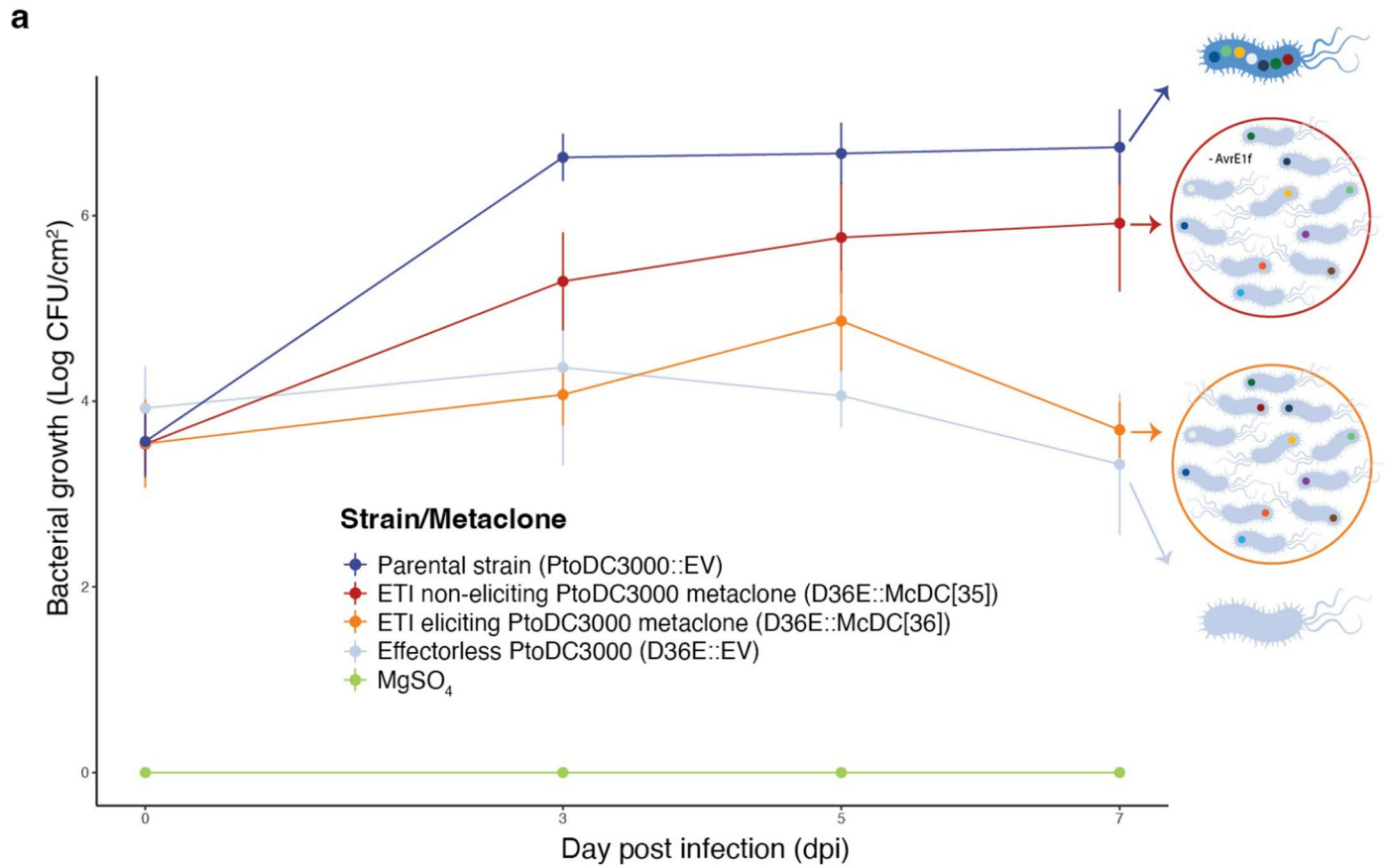
Extended Data Fig. 1 | In-planta fitness of individual effector clones. Bacterial growth was quantified on day 6 post spray-infection for at least 4 independent plant replicates infected with each of the 36 effector clones that comprise the well-expressed effector arsenal of the pathogen PtoDC3000. All infections were performed at the same time and controls were placed in each flat. D36E and PtoDC3000, each harboring an empty vector (EV), were used as negative and

positive virulence controls, respectively. No individual effector clone deviated significantly from the mean of the effector-less control strain. Elements in boxplots represent the median, 25th and 75th percentiles, and 1.5 * inter-quartile ranges. All comparisons were performed via one-way ANOVA with post-hoc Tukey-Kramer HSD using a 95% confidence interval (Source data and p-values provided in Supplementary Data 1).



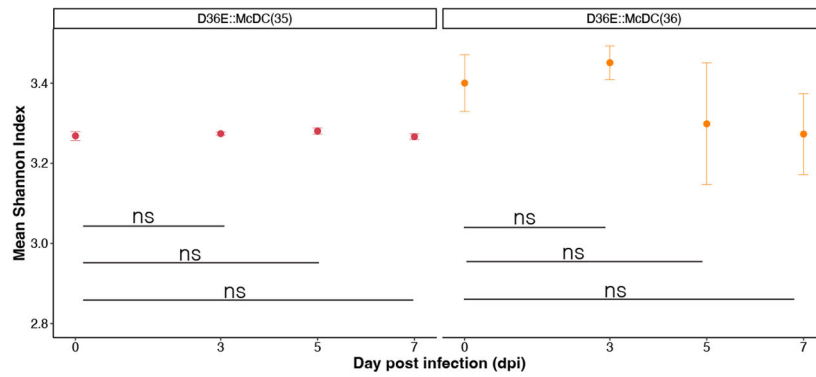
Extended Data Fig. 2 | In-vitro fitness of individual effector clones. Growth curves of individual effector clones composing the PtoDC3000 metaclone D36E::McDC[36], and control strains harboring empty vectors (EV). Harboring any of the individual effector plasmids did not substantially burden or benefit the growth of D36E *in vitro*. Data points represent the average optical density (OD) measured at 600 nm across 3 technical replicates grown in rich media

(KB) with kanamycin. Time measures with SE > 0.07 were excluded as the high variability was likely due to condensation, which was noticeable during lag phase, predominantly over the first 10 hours. This, however, did not impact the overall trajectory of the growth curves and there were no overall substantial differences between effector clones. NC: negative buffer control.



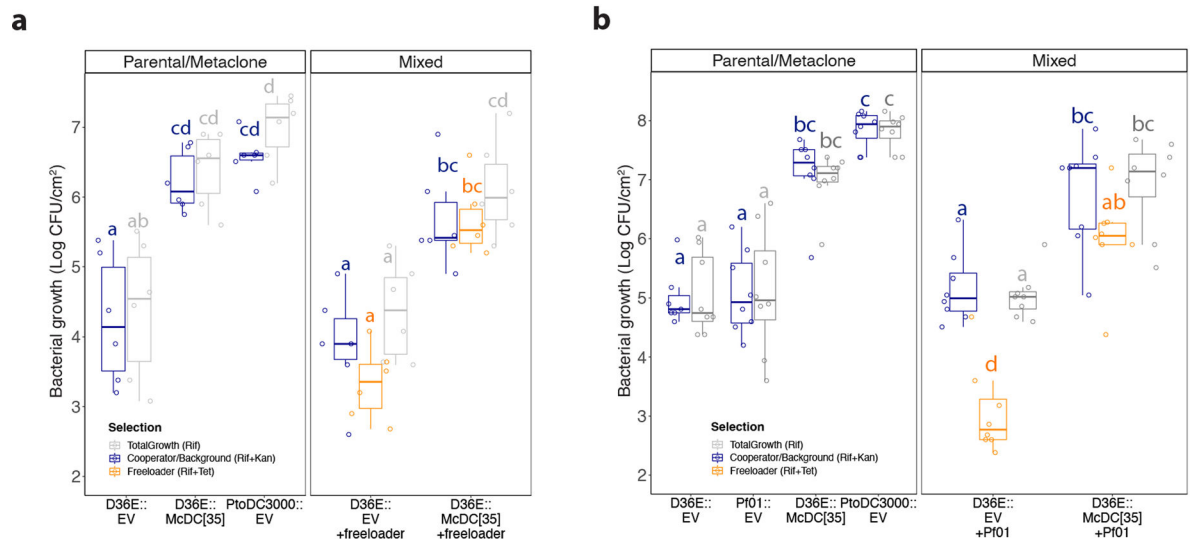
Extended Data Fig. 3 | Collective virulence emerges when using syringe pressure infiltration assays on *A. thaliana*. **a.** Endophytic bacterial growth at 0-, 3-, 5- and 7-days post infection using syringe pressure infiltration. Diagrams on the right represent the corresponding population and genetic makeup of each

infection. Error bars correspond to standard deviation from the mean of at least 4 biological replicates per treatment at each timepoint. **b-d.** Host symptoms shown in photos taken of 4 representative leaves per bacterial treatment, and 2 plants for MgSO₄ controls at **b**, 3-, **c**, 5- and **d**, 7- days post infection.



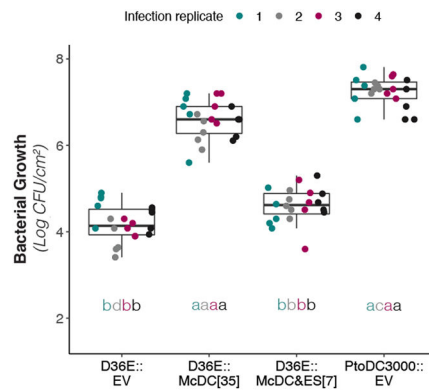
Extended Data Fig. 4 | Mean Shannon's diversity index for metaclones does not deviate significantly throughout disease progression. Diversity calculations were based on the relative abundance of each D36E::effector barcode composing the PtoDC3000 metaclones D36E::McDC[36] (ETI-eliciting) and D36E::McDC[35] (not ETI-eliciting). Barcode sequence diversity is reported as the mean Shannon index across four biological replicates \pm SE for each metaclone. No significant differences were found between any stage of infection and the mean barcode diversity of the original inoculum (Bonferroni-corrected

two-sided Student's t-tests. p-values: D36E::McDC[35]: D0pi-D3pi = 0.66, D0pi-D5pi = 0.41, D0pi-D7pi = 0.89; D36E::McDC[36]: D0pi-D3pi = 0.56, D0pi-D5pi = 0.57, D0pi-D7pi = 0.35). Error bars represent standard error across 4 biological replicates. Higher variance across replicates is observed in the ETI-eliciting metaclone D36E::McDC[36], particularly on the latter stages of the infection process, which can be attributed to smaller population sizes and increased drift in the metaclone composition.



Extended Data Fig. 5 | Freeloading strains benefit from collective virulence and coexist with cooperating portion of the metaclone. The virulent PtoDC3000 metaclone D36E::McDC[35] or mock population (D36E::EV) were mixed with strains unfit for multiplication in the plant apoplastic space (that is, freeloaders). Bacterial endophytic growth is reported at 7 dpi for cooperator and freeloader, separately and together, following standard spray infection of mixed populations and controls (**Fig2**). Differential antibiotic selection shown was used to measure fitness of the two genotypes present in each population, together (Total Growth – Rifampicin only -grey) and separately (Cooperator -rifampicin

and tetracycline -blue; Freeloader- rifampicin and kanamycin -orange) **a**. The effectless polymutant strain D36E, and **b**. the natural soil-associated sister species Pf0-1 are rescued to significantly higher load when in the presence of public goods provided cooperatively by the metaclone. Elements in boxplots represent the median of 6 biological replicates per treatment per selection category, the 25th and 75th percentiles, and 1.5 * inter-quantile ranges. Letters represent significant groups estimated via one-way ANOVA with post-hoc Tukey-Kramer HSD using a 95% confidence interval (Source data and p-values in in Supplementary Data 1).



Extended Data Fig. 6 | Metaclone representing the effector allele overlap between PtoDC3000 and PmaES4326, McDC&ES[7], fails to match fitness of PtoDC3000 and the non-ETI-eliciting metaclone D36E::McDC[35]. D36E::McDC&ES[7] shows a fitness significantly closer to that of the effectorless polymutant D36E::EV and does not restore the growth levels typical of their wildtype parental strain PtoDC3000 or its non-ETI eliciting metaclone

D36E::McDC[35]. *In-planta* fitness was quantified 6 dpi for 5 biological replicates per treatment and 4 independent infection replicates. Elements in boxplots represent the median, 25th and 75th percentiles, and 1.5 * inter-quantile ranges. Comparisons were performed via one-way ANOVA and post-hoc Tukey-Kramer HSD using a 95% confidence interval was performed separately for 4 independent experiments (Source data and p-values in Supplementary Data 1).

a



b

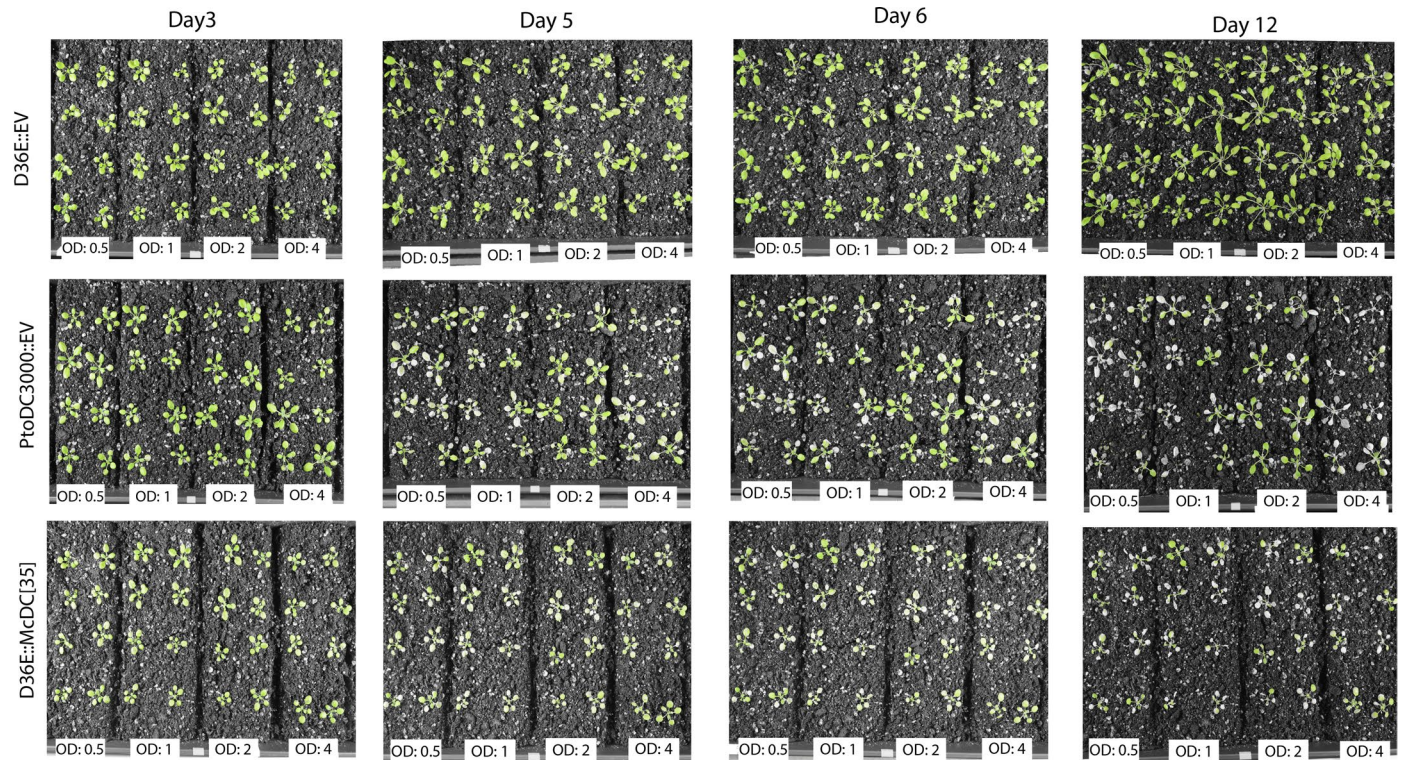


c



Extended Data Fig. 7 | Representative plant photos show symptom development for the metaclones D36E::McDC[35] and PfEtHA::McDC[35] compared to their effector-less background and the pathogen PtoDC3000. For each treatment, a total of 8 leaves from 2 plants show host symptoms at a. 3, b. 5, and c. 7 days post bacterial pressure infiltration. The progression of symptom development is visible in photos taken with a no-flash standard settings

(left panels) and with a camera green-pass effect filter setting which facilitates the inspection of lesions (grey) and viable (green) tissue (right panels). The MgSO₄ control, D36E::EV and PfEtHA::EV treatments are presented on the left (top to bottom), and PtoDC3000::EV, D36E::McDC[35] and PfEtHA::McDC[35] are presented on the right (top to bottom).



Extended Data Fig. 8 | Dose response of the PtoDC3000 metaclone D36E::McDC[35]. A range of inoculum concentrations (OD_{600} 0.5, 1, 2 and 4) was tested on 8 plants and visual symptoms were followed at 3, 5, 6 and 12 dpi. Photos were taken with a green-only pass filter, showing in grey any chlorotic yellow or brown tissue. Plant fitness (ie. green) detectably declines more when infected

with the pathogen PtoDC3000 and the D36E::McDC[35] than it does for the effectorless control D36E::EV. No visual differences are observed across the range of concentrations tested for the metaclone D36E::McDC[35] and plant fitness is visually reduced at an optical density as low as 0.5.

Reporting Summary

Nature Portfolio wishes to improve the reproducibility of the work that we publish. This form provides structure for consistency and transparency in reporting. For further information on Nature Portfolio policies, see our [Editorial Policies](#) and the [Editorial Policy Checklist](#).

Statistics

For all statistical analyses, confirm that the following items are present in the figure legend, table legend, main text, or Methods section.

n/a | Confirmed

- The exact sample size (n) for each experimental group/condition, given as a discrete number and unit of measurement
- A statement on whether measurements were taken from distinct samples or whether the same sample was measured repeatedly
- The statistical test(s) used AND whether they are one- or two-sided
Only common tests should be described solely by name; describe more complex techniques in the Methods section.
- A description of all covariates tested
- A description of any assumptions or corrections, such as tests of normality and adjustment for multiple comparisons
- A full description of the statistical parameters including central tendency (e.g. means) or other basic estimates (e.g. regression coefficient) AND variation (e.g. standard deviation) or associated estimates of uncertainty (e.g. confidence intervals)
- For null hypothesis testing, the test statistic (e.g. F , t , r) with confidence intervals, effect sizes, degrees of freedom and P value noted
Give P values as exact values whenever suitable.
- For Bayesian analysis, information on the choice of priors and Markov chain Monte Carlo settings
- For hierarchical and complex designs, identification of the appropriate level for tests and full reporting of outcomes
- Estimates of effect sizes (e.g. Cohen's d , Pearson's r), indicating how they were calculated

Our web collection on [statistics for biologists](#) contains articles on many of the points above.

Software and code

Policy information about [availability of computer code](#)

Data collection	ICG12 robot manufactured by S&P Robotics was used to collect optical density (600nm) for in-vitro growth curves. All in-planta bacterial growth was quantified via colony-counting in a stereoscope. Plant photos were taken using a Nikon D5200 DSLR camera, with a Nikon 18 to 140mm DX VR lens.
Data analysis	All data processing was performed in RStudio v.1.3.1073, using packages in tidyverse (v1.3.1), ggpubr (v0.4.0), multcompView (v0.1-8), vegan v.2.5-7, Biopython (v.1.79). Barcode data analysis was done with a script uploaded to DOI: 10.5281/zenodo.7249118 (https://zenodo.org/record/7249118). Trimmomatic (0.38) was used to remove sequencing adapters, filter (-phred33) and set minimal length (MINLEN:100).

For manuscripts utilizing custom algorithms or software that are central to the research but not yet described in published literature, software must be made available to editors and reviewers. We strongly encourage code deposition in a community repository (e.g. GitHub). See the Nature Portfolio [guidelines for submitting code & software](#) for further information.

Data

Policy information about [availability of data](#)

All manuscripts must include a [data availability statement](#). This statement should provide the following information, where applicable:

- Accession codes, unique identifiers, or web links for publicly available datasets
- A description of any restrictions on data availability
- For clinical datasets or third party data, please ensure that the statement adheres to our [policy](#)

The datasets generated /analyzed during the current study are available in Extended Data/Supplement files and any additional information can be provided upon request

Human research participants

Policy information about [studies involving human research participants and Sex and Gender in Research](#).

Reporting on sex and gender

NA

Population characteristics

NA

Recruitment

NA

Ethics oversight

NA

Note that full information on the approval of the study protocol must also be provided in the manuscript.

Field-specific reporting

Please select the one below that is the best fit for your research. If you are not sure, read the appropriate sections before making your selection.

Life sciences Behavioural & social sciences Ecological, evolutionary & environmental sciences

For a reference copy of the document with all sections, see [nature.com/documents/nr-reporting-summary-flat.pdf](https://www.nature.com/documents/nr-reporting-summary-flat.pdf)

Life sciences study design

All studies must disclose on these points even when the disclosure is negative.

Sample size

Sample sizes were chosen considering the feasibility of experimental manipulation while maintaining biological, technical and experimental replication. We used sample sizes that are very consistent with those used in our field that balance the required statistical power with the available growth space.

Data exclusions

No data was excluded

Replication

In-planta experiments consisted of a minimum of 4 biological replicates per treatment and each biological replicate. For each biological replicate, 4 plant disks were harvested and pooled. All replicates are shown and any discrepancies are described in the text.

Randomization

A. thaliana ecotype Col-0 seeds were collected and sterilized in the lab. This bulking has shown homogeneous results, therefore would not require randomization. Same principle applies for microbial strains, which were stocked clonally from single colonies.

Blinding

Explicit blinding is not typically done with plant pathology assays although infections, sampling, processing, and reading is done without respect to the specific interaction being assayed and much of the data collection is automated.

Reporting for specific materials, systems and methods

We require information from authors about some types of materials, experimental systems and methods used in many studies. Here, indicate whether each material, system or method listed is relevant to your study. If you are not sure if a list item applies to your research, read the appropriate section before selecting a response.

Materials & experimental systems

n/a	Involvement in the study
<input checked="" type="checkbox"/>	<input type="checkbox"/> Antibodies
<input checked="" type="checkbox"/>	<input type="checkbox"/> Eukaryotic cell lines
<input checked="" type="checkbox"/>	<input type="checkbox"/> Palaeontology and archaeology
<input checked="" type="checkbox"/>	<input type="checkbox"/> Animals and other organisms
<input checked="" type="checkbox"/>	<input type="checkbox"/> Clinical data
<input checked="" type="checkbox"/>	<input type="checkbox"/> Dual use research of concern

Methods

n/a	Involvement in the study
<input checked="" type="checkbox"/>	<input type="checkbox"/> ChIP-seq
<input checked="" type="checkbox"/>	<input type="checkbox"/> Flow cytometry
<input checked="" type="checkbox"/>	<input type="checkbox"/> MRI-based neuroimaging